



Swansea University
Prifysgol Abertawe



Cronfa - Swansea University Open Access Repository

This is an author produced version of a paper published in:

Clinical & Experimental Ophthalmology

Cronfa URL for this paper:

<http://cronfa.swan.ac.uk/Record/cronfa50970>

Paper:

Churm, R., Dunseath, G., Prior, S., Thomas, R., Banerjee, S. & Owens, D. (2019). Development and characterization of an in vitro system of the human retina using cultured cell lines. *Clinical & Experimental Ophthalmology*

<http://dx.doi.org/10.1111/ceo.13578>

This item is brought to you by Swansea University. Any person downloading material is agreeing to abide by the terms of the repository licence. Copies of full text items may be used or reproduced in any format or medium, without prior permission for personal research or study, educational or non-commercial purposes only. The copyright for any work remains with the original author unless otherwise specified. The full-text must not be sold in any format or medium without the formal permission of the copyright holder.

Permission for multiple reproductions should be obtained from the original author.

Authors are personally responsible for adhering to copyright and publisher restrictions when uploading content to the repository.

<http://www.swansea.ac.uk/library/researchsupport/ris-support/>

1 Development and characterization of an
2 *in vitro* system of the human retina
3 using cultured cell lines
4

5 Churm R. PhD¹, Dunseath GJ. PhD¹, Prior SL. PhD¹, Thomas RL. PhD¹, Banerjee S. PhD²,

6 Owens DR. MD¹

7 ¹Diabetes Research Group, Grove Building, Swansea University, Swansea, UK

8 ²Cardiff and Vale Health Board, University of Wales Hospital, Cardiff, UK

9 **Running title**

10 Novel triple-culture of the human retina

11

12

13 **Conflicts of interest-** None.

14 **Funding Source-** St David's Medical Foundation

15 **Correspondence**

16 Dr Rachel Churm

17 Tel: +44(0)1792 602310

18 Email: r.churm@swansea.ac.uk

19

20 **Abstract**

21 **Background:** Previously developed *in vitro* cultures of the human retina have been solo
22 or dual cell cultures. We developed a triple-cell culture *in vitro* model utilizing a
23 membrane system to produce a better representation of a functional and morphological
24 human retina.

25 **Methods:** Retinal microvascular endothelial cells (HRMVEC/ACBRI181, Cell systems),
26 retinal pigment epithelium cells (RPE/ARPE-19, ATCC) and Müller glial cells (MIO-M1,
27 UCL) were grown in a triple-culture. Our optimized triple-culture media contained a mix
28 of specific endothelial medium and high glucose Dulbecco's Modified Eagle's medium
29 (DMEM), where all three layers were viable for up to 5 days. Co-culture effect on
30 morphological changes (cell staining) and gene expression of functional genes (pigment
31 epithelial derived factor (*PEDF*) and vascular endothelial growth factor (*VEGF*)) were
32 measured from RNA via real time PCR. Expression of tight junction protein 1 (*TJP1*) was
33 measured in RNA isolated from ARPE-19s, to assess barrier stability.

34 **Results:** The triple-culture promotes certain cell functionality through up-regulation of
35 *TJP1*, increasing *PEDF* and decreasing *VEGF* expression highlighting its importance for
36 the assessment of disease mechanisms distinct from a solo culture which would not
37 allow the true effect of the native microenvironment to be elucidated.

38 **Conclusion:** This model's novelty and reliability allows for the assessment of singular
39 cellular function within the retinal microenvironment and overall assessment of retinal
40 health, whilst eliminating the requirement of animal-based models.

41 **Key words;** Human retina, Cell culture, Triple-culture, *In vitro* model

42

43 **1. Introduction**

44 The human eye is a complex organ that is comprised of three main areas; the cornea,
45 lens, and the retina. The retina is a highly specialised organ of photoreception, involved
46 in translating light energy into action potentials which are relayed to the brain, where
47 the information is processed into vision. The integrity of the retina is dependent upon
48 its immediate microenvironment, which is reliant on cell-cell interactions of the
49 different human retinal cellular components. Disruption of which results in a variety of
50 retinal diseases including diabetic retinopathy (DR)¹. DR is associated with the
51 breakdown of both the inner blood-retinal-barrier (BRB)^{2,3} and more recently linked to
52 the outer BRB⁴. The inner BRB is composed of tight junctions between retinal capillary
53 endothelial cells and the outer of tight junctions between the retinal pigment epithelial
54 cells (RPE). The inter-relationship between vascular and endothelial cells that form the
55 BRB is vital maintaining a specialized environment of the neural retina.

56 Current findings show that BRB breakdown is multifactorial, including; impaired
57 endothelial cells, pericyte demise, thickening of capillary basement membrane and the
58 alteration of tight junctions between RPE and endothelial cells⁵. Additionally RPE,
59 endothelial and other cell types within the retina can be responsible for the release of
60 neurotrophic factors that can alter the integrity of the BRB, such as vascular endothelial
61 growth factor (VEGF) and pigment endothelial derived factor (PEDF)⁶⁻⁸. These factors
62 can also be released from Müller cells⁸⁻¹⁰, which are a subset of the retinal macroglia
63 that are strongly linked to RPEs, establishing structural connections with the subretinal
64 space and choroidal vasculature^{8, 11}. It is evident that research into DR requires a

65 complex system that can encompass the interaction of all cells present within both the
66 inner and outer BRB.

67 Currently research into retinal disease utilizes two main methodologies; *in vitro*
68 analysis of solo or dual cell cultures, and animal models. The current literature and
69 project designs relating to RPE cultures are often limited to them encompassing a dual-
70 culture system with endothelial cells. The culture formations published comprise of cells
71 either in direct contact¹², sandwiched with extracellular matrix proteins^{13, 14}, or cells
72 cultured on either side of a membrane¹⁵⁻¹⁷. Alternatively, there are published models
73 that encompass a dual system where these cells do not come into contact¹⁸. There are
74 very few multi-culture systems within literature, with those published comprising of
75 mixed species cell sources¹⁹. We aim to expand on current *in vitro* models to develop a
76 triple-culture which utilizes both human cell lines and primary cells, to demonstrate a
77 better representation of a functional and morphological human retina.

78

79 **2. Methods**

80 **Cell line and isolated primary cell culture**

81 **Retinal pigment epithelial cells**

82 RPE were authenticated and sourced as a commercially available cell line; ARPE-19
83 (ATCC® CRL-2302, USA). Upon receipt were grown in Dulbecco's Modified Eagle's
84 medium (DMEM) containing glutamine supplemented with 10% fetal bovine serum
85 (FBS) and 1% penicillin-streptomycin (Invitrogen-Gibco, Rockville, MD). Cells were

86 incubated at 37°C at 5% CO₂, with media changed every 2-3 days and sub-cultured (1:3
87 split) at 80% confluency with 0.05% trypsin-EDTA (Invitrogen-Gibco, Rockville, MD).

88 **Müller glial cells**

89 Human Moorfield Institute of Ophthalmology-Müller 1 (MIO-M1) cell line were isolated,
90 authenticated and purchased from Professor Limb (Institute of Ophthalmology and
91 Moorfields Eye Hospital, UK)²⁰. Upon arrival, cells were cultured in the same media as
92 ARPE-19, incubated at 37°C at 5% CO₂ and media changed every 2-3 days.

93 **Retinal microvascular endothelial cells**

94 Primary human retinal microvascular endothelial cells (HRMVEC) are commercially
95 available, sourced from Applied Cell Biology Research Institute (ACBRI 181, Cell Systems,
96 Kirkland, USA). All experimental procedures completed using primary cells were in
97 compliance with the Human Tissue Act. Cells were grown in Cell Systems Culture (CS-C)
98 medium, incubated at 37°C at 5% CO₂, with media changed every 2-3 days. Cells were
99 passaged when confluent using Cell Systems Passage Reagent (all reagents sourced from
100 Cell Systems, Kirkland, USA) and used in experiments at passage 8.

101

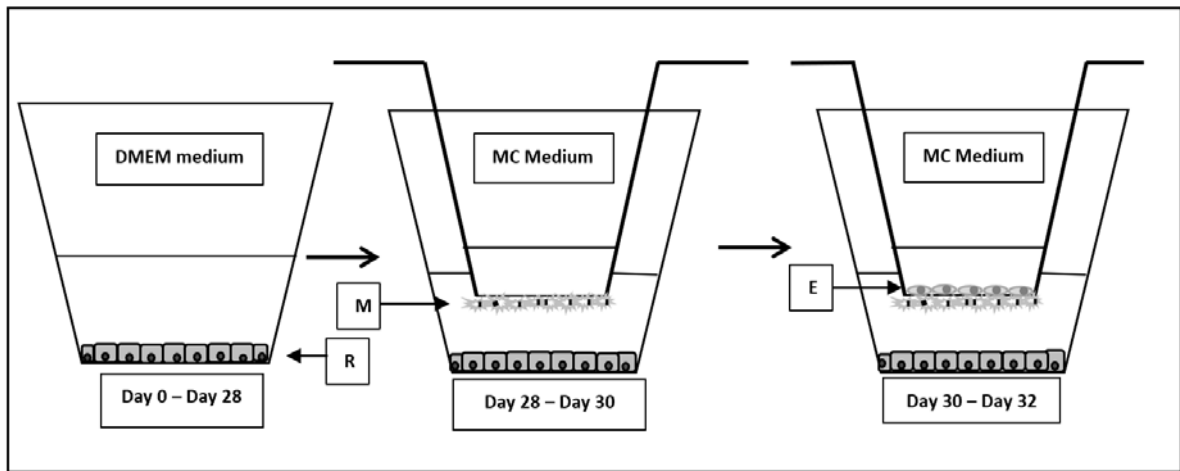
102 **Co-culture formation**

103 To assess cell viability in a microenvironment, cells were grown in solo, dual (MIO-M1 &
104 ARPE-19, ARPE-19_& HRMVEC and MIO-M1 & HRMVEC)_and triple formations (ARPE-19,
105 MIO-M1 & HRMVEC), using the following protocol.

106

107 **System set-up**

108 During solo-, dual- and triple-culture formations all cell types were grown in the same
109 location as seen within triple-culture schematic (Figure 1). Multi-culture system utilizes
110 a 0.4 μm pore size polyester (PET) Transwell® membrane with a 10 μm membrane
111 thickness (Corning, Thermo Scientific, UK). Cells were plated according to Figure 1, using
112 an in-house optimized multi-culture media (MC media) consisting of 2:1 DMEM with
113 glutamine: CS-C medium.



114
115 **Figure 1.** Triple-culture schematic for ARPE-19 (R), MIO-M1 (M) and HRMVEC (E). Annotated medium is
116 the culturing medium present in both well insert and culture dish well as described in methodology, multi-
117 culture. (MC).

118

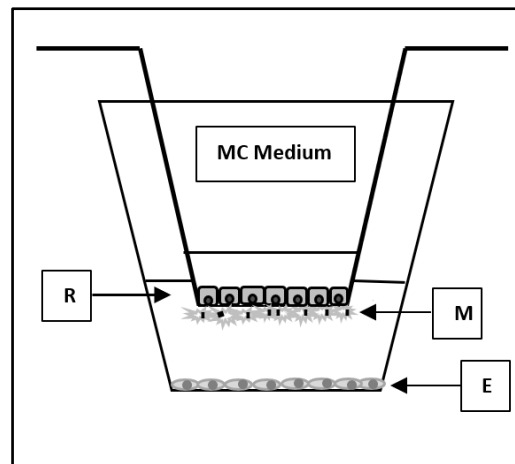
119 **Cell seeding and maturation**

120 ARPE-19 was grown on the base of a 6-well culture dish, as shown (Figure 1). Cells were
121 prepared for all experiments at passage 6, split ratio 1:3, requiring maturation and tight-
122 junction formation for 28 days with growth media changed every 2-3 days (Supp. Figure
123 1A). At day 28, MIO-M1 cells were seeded at 100,000 cells per cm^2 in 150 μL (passage
124 34) onto the basal side of a Transwell® membrane by inverting the membrane structure
125 and incubated for 3 hours at 37°C at 5% CO_2 . Once adhered, excess medium was

126 removed, the membrane reversed and placed in the 6-well culture plate containing the
127 ARPE-19 cells. At day 32, HRMVEC were seeded at 100,000 cells per cm² to the apical
128 surface of the membrane insert washed with attachment factor, and grown in 1.5 mL
129 MC medium, cells reached optimal confluency (70%) for experimentation after 48 hours
130 (day 34). MC media of well and insert was replenished every 2-3 days, cell viability valid
131 for up to 5 days of construction of complete model (i.e. day 37) due to cellular
132 characteristics and phenotypes of specific cell lines being lost after prolonged culture (>
133 14 days)²⁰.

134 For permeability assay, an alternative layout was assembled to assess barrier
135 properties as original triple-culture layout does not allow for this. Cells were cultured as
136 described previously, but with cell seeding and maturation occurring in alternative
137 positions i.e. ARPE-19 grown on apical surface of the membrane, MIO-M1 on basal
138 surface and HRMVEC on bottom of the culture well (Figure 2).

139



140

141 **Figure 2.** A- Alternative formation of multi-culture to assess Transwell® permeability in a multi-culture. R-
142 ARPE-19, M-MIO-M1 and E-HRMVEC.

143

144 **Morphological changes**

145 Immunocytochemical analysis was conducted to ensure the presence of correct cell
146 types within culture (See Supp. Work 1 and Supp. Figure 1). Basic cell morphologies and
147 relative diameter were determined using Hematoxylin (Sigma) staining and digital
148 imaging via light microscopy. Cell quantification, density and diameter were assessed
149 using ImageJ software (NIH, Version 2). Limitations of a basic cell imaging only allows
150 data to be used as a relative check for cell morphology instead of a quantification of
151 absolute size. Each experimental well produced images in 5 fields, each field was pre-
152 defined and set prior to cell seeding to remove experimental bias. A total of 20 cells per
153 type at x50 magnification were analysed to determine cell diameter and morphologies
154 (n=100 cells for data analysis, per biological repeat) (representation of images provided
155 in Supp. Figure 2). Each cell type was analysed within 3 biological repeats.

156

157 **Gene expression analysis**

158 All expression data was collected from each culture layout from three biological repeats
159 and three experimental repeats per plate (n=9 per culture layout). Individual cells types
160 were harvested at day 32 of culture, homogenized in QIAzol lysis reagent and total RNA
161 isolated using a RNeasy Mini Kit (Qiagen, UK). 1000ng/ μ l of total RNA was converted to
162 cDNA using a reverse transcription kit (Invitrogen, Thermo Fisher, UK). 1:10 dilutions of
163 cDNA transcripts were run on a CFX connect (BioRad, UK) using SYBR Green I (BioRad,
164 UK) for each primer set (**VEGF**: Forward-ACT TCT GGG CTG TTC TC, Reverse-TCC TCT TCC
165 TTC TCT TCT TCC; **PEDF**: Forward-TGC AGG CCC AGA TGA AAG GG, Reverse-TGA ACT CAG

166 AGG TGA GGC TC. **TJP1**: sourced and optimized from BioRad, UK) at optimal cycling
167 conditions of; 95°C for 3min, followed by 35 cycles of 95°C for 30s, 59.5°C for 30s and
168 72°C for 30s, followed by melt peak conditions. The average Ct value was
169 taken from triplicate assays and normalised against the invariant expression of β -
170 *actin* housekeeper gene. Result were analysed using the $2^{-\Delta\Delta Ct}$ method to produce
171 relative fold change values in comparison between groups, standard error of the mean
172 (SEM) was calculated from the average Ct value for each sample produced within the
173 experiment cohort. Fold change range of -1.5 to 1.5 is indicative of no overall change in
174 gene expression levels.

175

176 **Permeability assay**

177 Permeability assays were completed to assess barrier properties in a mixed cell
178 environment, based on a horseradish peroxidase (HRP) (Sigma™) diffusion ELISA (n=9,
179 per culture layout). For permeability assays, DMEM without FCS was used at all stages.
180 An alternative layout of both dual- and triple-culture was used to assess Transwell®
181 permeability due to the functional properties of each cell type. To assess the implication
182 of culture formation on both ARPE-19 and HRMVEC, they were grown on the apical and
183 basal side of the membrane, respectively. Medium within the well and insert
184 compartments were replaced for assay media and the insert compartment dosed with
185 HRP [1250 mU], incubated for 20 minutes and medium from the lower well
186 compartment collected for analysis. Culture media was transferred to a 96-well clear
187 microplate plate for colorimetric analysis via 3,3',5,5'-Tetramethylbenzidine (TMB) and
188 stop solution (Invitron, UK) and absorbance recorded at a wavelength of 450 nm and

189 corrected at 620 nm. Membrane permeability was analysed in comparison to a control
190 membrane with no cellular growth. Relative permeability was produced as a
191 percentage;

$$192 \quad \text{Relative Permeability (\%)} = \frac{\text{Culture Experiment Value}}{\text{Control Value}} \times 100$$

193

194 **Statistical analysis**

195 Raw data was analysed using SPSS™ Version 23. Continuous data is summarized by mean
196 and standard deviation (SD) when normally distributed, and by median and interquartile
197 range (IQR) if not normally distributed. Normality of the data was verified by the
198 Kolmogorov-Smirnov test and visualised on q-q plots. A Student t-test was used to
199 compare the mean of two groups and analysis of variance (ANOVA) to compare the
200 mean of more than two groups for normally distributed data. Alternatively, not normally
201 distributed data was analysed using Mann Whitney U and Kruskal Wallis tests. For gene
202 expression data, statistical analysis was run on threshold cycle (Ct) data normalised
203 against *β-actin* housekeeper, assessed using Student t-test. P-values less than 0.05 were
204 deemed statistically significant.

205

206 **3. Results**

207 Cell morphology

208 Across all three cell types, no significant alterations in cell morphologies were noted in
209 any culture formation (Table 1). Analysis of HRMVEC morphologies using cellular
210 staining and microscopy was unable to produce sufficient images within the triple-
211 culture to assess cell diameter. RNA spectroscopy did confirm cell growth on the apical

212 surface and we believe a lack of imaging reflect limitations within methodology. Gene
 213 expression of *TJP1* was measured in RNA isolated from ARPE-19 to assess barrier stability
 214 in a multi-culture system. Data indicates a significant increase in fold change (FC) for
 215 *TJP1* when RPE are grown in combination with either MIO-M1 (+11.4 FC, p<0.001),
 216 HRMVEC (+12.9 FC, p<0.001) or both in a triple-culture (+7.8 FC, p<0.001) (Figure 3).
 217 Barrier permeability was not assessed within the primary formation of the dual- and
 218 triple-culture as described in methodology.

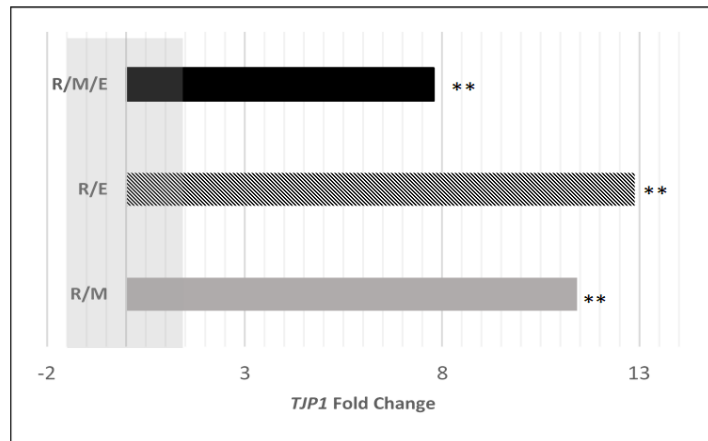
219

220 **Table 1.** Mean and standard deviation of cell diameter (μM) for the three cell types grown in all culture
 221 formations. P-value determined using one-way ANOVA.

222

Culture Formation	Cell Type		
	<u>ARPE-19</u> (n=300)	MIO-M1 (n=300)	HRMVEC (n=300)
Solo	17.5 (6.1)	62.7 (13.3)	98.9 (24.4)
Dual		61.9 (10.6)	97.8 (28.0)
Dual	18.1 (4.3)		96.0 (22.9)
Dual	17.9 (4.5)	63.8 (13.9)	
Triple	18.2 (5.3)	62.5 (14.3)	-
P-value	0.48	0.54	0.66

232



233

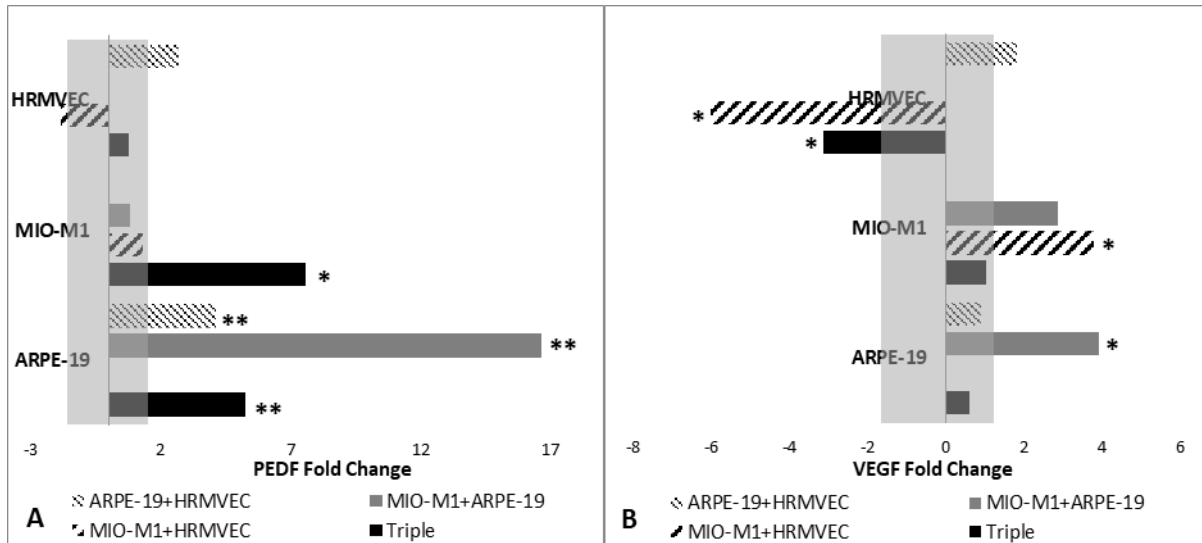
234 **Figure 3.** Relative fold change values for *TJP1* gene expression data in multi-culture formations in
 235 comparison to solo-culture. Fold change between -1.5 and 1.5 is classed as no relative gene expression
 236 change (grey shaded region). Statistical significance represented by asterisks (** $p < 0.01$), determined
 237 using an independent t-test. R-ARPE-19, M-MIO-M1 and E-HRMVEC.

238

239 *Implications of multi-culture on gene expression levels*

240 *PEDF* expression (Figure 4A) demonstrated an increase in FC in both ARPE-19 (+5.2 FC,
 241 $p < 0.01$) and MIO-M1 (+7.5 FC, $p < 0.05$) in triple compared to solo-culture. Triple
 242 compared to solo-culture demonstrated no significant FC in *VEGF* expression in either
 243 MIO-M1 (+1.0 FC, $p = 0.49$) or ARPE-19 (+0.6 FC, $p = 0.34$) (Figure 4B). However, expression
 244 was significantly decreased within HRMVEC (-3.2 FC, $p < 0.05$). Sub-analysis of dual-
 245 cultures implicates MIO-M1 for the observed change in *VEGF* expression (dual-culture
 246 of; MIO-M1+HRMVEC, -6.0 FC, $p < 0.05$ and dual-culture; ARPE-19+HRMVEC, +1.80 FC,
 247 $p = 0.11$).

248



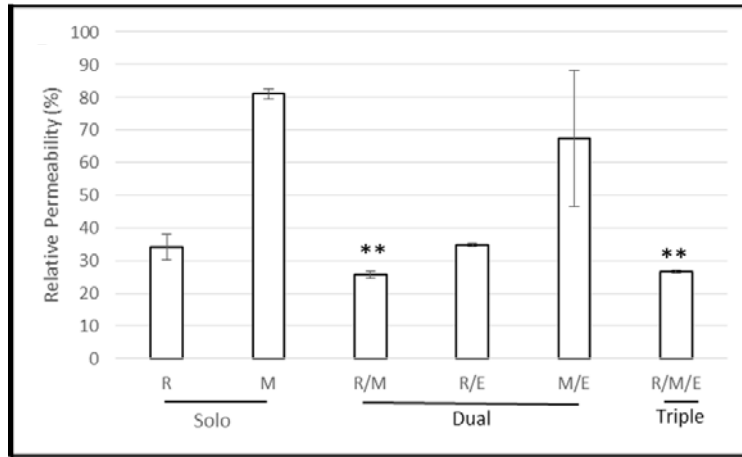
249

250 **Figure 4A-B.** Relative fold change values for gene expression data in multi-culture formations in
 251 comparison to solo-culture. Fold change between -1.5 and 1.5 is classed as no relative gene expression
 252 change (grey shaded region). (A) *PEDF*-fold change & (B) *VEGF*-fold change. Statistical significance
 253 represented by asterisks (* $p < 0.05$, ** $p < 0.01$), determined using an independent t-test of the difference
 254 of ΔCt in multi-culture formation of cells versus solo-cultured cells.

255

256 *Assessment of multi-culture on membrane properties*

257 HRP diffusion across the Transwell® membrane altered significantly dependent on the
 258 cells grown on the surface. ARPE-19 monolayer formation resulted in the diminishing of
 259 HRP passing through the membrane, this barrier was significantly strengthened in the
 260 presence of MIO-M1 grown on the basal side of the membrane in both a dual- and triple-
 261 culture (ARPE-19 vs ARPE-19/MIO-M1; 34.1 (3.9)% v 25.7 (1.2)%: $p < 0.01$; ARPE-19 vs
 262 ARPE-19/MIO-M1/HRMVEC; 34.1 (3.9)% vs 26.5 (0.5)%: $p < 0.01$) (Figure 5). Diffusion of
 263 molecules through the Transwell® membrane is significantly reduced by cell growth on
 264 the surface, data demonstrated minimal relative permeability is 25.7% (± 1.2) indicating
 265 cross membrane molecule diffusion is still occurring.



266

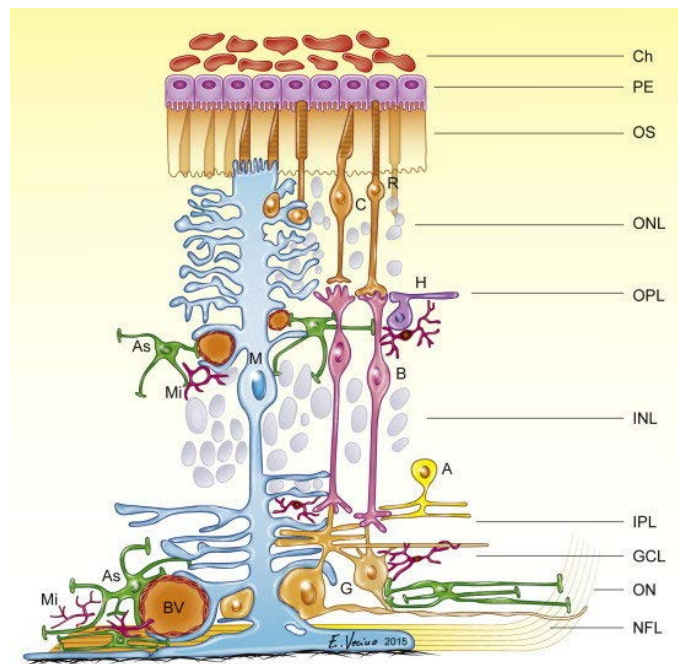
267 **Figure 5.** HRP diffusion assay, relative permeability (%) for all cell formations that require growth on the
 268 Transwell® membrane, error bars indicate standard deviation. Statistical significance represented by
 269 asterisks (** $p < 0.01$), determined using an independent t-test. R-ARPE-19, M-MIO-M1 and E-HRMVEC.

270

271 4. Discussion

272 This study presents the evidence for a novel human *in vitro* model of the retina. This
 273 model is reproducible and provides flexibility in formation and structure to maximise
 274 the yield of experimental research that can be conducted, including mechanistic
 275 research into retinal disease, retina biology and pharmacology intervention. The culture
 276 model allows for the arrangement of cellular components that mimic the retinal
 277 microvasculature, neuronal retina and RPE *in vivo*, allowing us to explore the tissues
 278 cellular microenvironment. The triple-culture model represents the close contacting
 279 relationship between the Müller glial cells (MIO-M1) and the blood vessels (HRMVEC)
 280 within the retina and the distal location of the non-contacting RPE (ARPE-19) retinal
 281 layer (Figure 6)²¹. These cell types in particular play a pivotal role in the function of the
 282 BRB and investigation of their cross-communication could lead to great enhancements
 283 for understanding retinal disease that results in, or is the result of, BRB malfunction.

284 Our findings highlight the importance of cell to cell interaction in retinal biology,
 285 with multi-culture systems resulting in changes in both structural and genetic alterations
 286 when compared to solo-cultures. On the other hand, the assessment of cell morphology
 287 resulted in no significant changes when the cells were grown in solo or in formations
 288 with each other. However, the methodology used to assess morphology is a basic
 289 technique and is limited in quantification and should only be utilised as an indication of
 290 cell type presence. We propose that within future expansion of this model, investigation
 291 into an optimized confocal analysis of cell markers across the membrane will confirm
 292 and quantify our original findings.



293
 294 **Figure 6.** Schematic drawing of the cellular components of the retina taken from Vecino *et al*, 2016²¹. The
 295 different cell types are situated in a standard large mammalian retina, depicting the interactions between
 296 the Müller cells in blue (M) and blood vessels (BV) (represented in triple-culture model with HRMVEC).
 297 Different layers of the retina; optic nerve (ON), nerve fibre layer (NFL), ganglion cell layer (GCL), inner
 298 plexiform layer (IPL), inner nuclear layer (INL), outer plexiform layer (OPL), outer nuclear layer (ONL), outer
 299 segment layer (OS), retinal pigment epithelium (RPE) & choroid (Ch).

300 Structurally, these findings indicate a significant 11- and 7-fold increase in gene
301 expression for *TJP1* or often referred to as zonula occludens (ZO1), when RPE are grown
302 in either a solo-culture, or in combination with MIO-M1 as a dual-culture or in a triple-
303 culture. This is also reflected within the barrier properties of the cultures, indicating a
304 significantly strengthened barrier when MIO-M1 cells were grown on the basal side of
305 the membrane. Previously published findings have associated Müller glial cell with
306 tightened tight junctions and upregulated and polarized localization of specific blood-
307 brain-barrier transporters^{19, 22}. However, expansion of these findings would require
308 protein analysis to determine the downstream impact.

309 Within DR and retinal disease, often researched is the alteration of key genes.
310 Gerhardinger and colleagues report that in mice, 6 months post streptozotocin
311 induction of diabetes, resulted in the alteration of 78 genes within Müller glial cells²³.
312 Over a third of these genes were reported to be associated with inflammation and
313 inflammatory response including cytokines such as VEGF^{5, 23}. These inflammatory
314 cytokines can initiate a cascade of events within the retinal microenvironment and result
315 in dysfunction of various cell types. The findings of this model indicate that within a
316 triple-culture, expression of *VEGF* was significantly altered within HRMVEC; we
317 hypothesise this is due to the presence of MIO-M1 cells. *PEDF* expression is often
318 demonstrated in literature to promote the health of the BRB^{24, 25}; within this model we
319 show a marked increase in *PEDF* gene expression. We hypothesise that the triple-culture
320 system promotes the functionality of the BRB, not only structurally through the
321 promotion of *TJP1/ZO1*, but also by an increase in the expression of beneficial growth
322 factors such as *PEDF* and decreasing the expression of detrimental growth factors such

323 as *VEGF*. This data highlights the significance of using a multi-culture system within the
324 assessment of disease mechanism, as a solo-culture would not elucidate the effect of
325 the native environment due to the implications of additional cell types. Let alone this
326 model does not represent all cell types present within the retina, it does provide species
327 specificity and three cell type interactions, therefore improving on the current retinal
328 models available and published.

329 Often disputed in literature, is the use of cell lines in model design due to the
330 presence of developmental abnormalities^{17, 26}. The prolonged culture of both ARPE-19
331 and MIO-M1 can result in abnormalities in characteristic features of the cell such as the
332 loss of pigmentation in ARPE-19 and MIO-M1 exhibiting progenitor characteristics²⁷.
333 However, within our study design we have allowed for maturation and low passage
334 numbers to ensure manipulation of culture conditions will result in minimal difference
335 from parent tissue²⁶. The superior use of an alternative cell source i.e. primary cell
336 sources will yield a truer representation of the native tissue. However, it can also
337 produce poor efficiency of the model in practice allowing for restricted use of repeats
338 and minimise use in pharmacological testing. Additionally, models do not allow for the
339 manipulation of culture environments to exacerbate a disease effect, for example;
340 chronic exposure to high glucose and varying glycaemic levels during cell seeding and
341 growth, to induce phenotypes seen in DR. Due to difficulties in sourcing human primary
342 cells for the modelling of the retina, to date only a rodent *in vitro* model¹⁹ and no human
343 multi-culture system have been published. We propose the compromise of two highly
344 characterized and routinely used cell lines ARPE-19²⁸⁻³⁰ and MIO-M1^{20, 27}; and one
345 primary sourced cell origin ACBRI-181 within this model, allowed for an *in vitro* multi-

346 culture model to be utilized in place of either an *in vitro* mixed species model or an *in*
347 *vivo/in vitro* animal model.

348 In conclusion, our methodology provides evidence for a novel multi-cell *in vitro*
349 culture model of the human retina, for the assessment of retinal biology and disease
350 mechanisms. The versatility of the model allows the assessment of both singular cellular
351 function within the retinal microenvironment in addition to a triple-cell assessment of
352 retinal structure and function in health and disease.

353

354

355 **Acknowledgement**

356 We would like to express a great gratitude to the St David's Medical Foundation for
357 funding this project.

358

359 References

- 360 [1] Simo R, Hernandez C: Novel approaches for treating diabetic retinopathy based on recent
361 pathogenic evidence. *Progress in Retinal and eye Research* 2015, 48:160-80.
- 362 [2] Frey T, Antonetti DA: Alterations to the blood–retinal barrier in diabetes: cytokines and
363 reactive oxygen species. *Antioxidants & redox signaling* 2011, 15:1271-84.
- 364 [3] Zhang X, Zeng H, Bao S, Wang N, Gillies MC: Diabetic macular edema: new concepts in patho-
365 physiology and treatment. *Cell & bioscience* 2014, 4:27.
- 366 [4] Daruich A, Matet A, Moulin A, Kowalczuk L, Nicolas M, Sellam A, Rothschild P-R, Omri S, Gélizé
367 E, Jonet L: Mechanisms of macular edema: beyond the surface. *Progress in retinal and eye
368 research* 2017.
- 369 [5] RübSam A, Parikh S, Fort P: Role of inflammation in diabetic retinopathy. *International journal
370 of molecular sciences* 2018, 19:942.
- 371 [6] Miller JW, Adamis AP, Shima DT, D'Amore PA, Moulton RS, O'Reilly MS, Folkman J, Dvorak
372 HF, Brown LF, Berse B: Vascular endothelial growth factor/vascular permeability factor is
373 temporally and spatially correlated with ocular angiogenesis in a primate model. *The American
374 journal of pathology* 1994, 145:574.
- 375 [7] Ferrara N, Davis-Smyth T: The biology of vascular endothelial growth factor. *Endocrine
376 reviews* 1997, 18:4-25.
- 377 [8] Sorrentino FS, Allkabes M, Salsini G, Bonifazzi C, Perri P: The importance of glial cells in the
378 homeostasis of the retinal microenvironment and their pivotal role in the course of diabetic
379 retinopathy. *Life sciences* 2016, 162:54-9.
- 380 [9] Fu S, Dong S, Zhu M, Sherry DM, Wang C, You Z, Haigh JJ, Le Y-Z: Müller glia are a major
381 cellular source of survival signals for retinal neurons in diabetes. *Diabetes* 2015:db150180.
- 382 [10] Nishikiori N, Osanai M, Chiba H, Kojima T, Mitamura Y, Ohguro H, Sawada N: Glial Cell–
383 Derived cytokines attenuate the breakdown of vascular integrity in diabetic retinopathy.
384 *Diabetes* 2007, 56:1333-40.
- 385 [11] Bringmann A, Pannicke T, Grosche J, Francke M, Wiedemann P, Skatchkov SN, Osborne NN,
386 Reichenbach A: Müller cells in the healthy and diseased retina. *Progress in retinal and eye
387 research* 2006, 25:397-424.
- 388 [12] Dardik R, Livnat T, Halpert G, Jawad S, Nisgav Y, Azar-Avivi S, Liu B, Nussenblatt RB,
389 Weinberger D, Sredni B: The small tellurium-based compound SAS suppresses inflammation in
390 human retinal pigment epithelium. *Molecular vision* 2016, 22:548.
- 391 [13] Fan W, Zheng JJ, McLaughlin BJ: An in vitro model of the back of the eye for studying retinal
392 pigment epithelial-choroidal endothelial interactions. *In Vitro Cellular & Developmental Biology-
393 Animal* 2002, 38:228-34.
- 394 [14] Sakamoto T, Sakamoto H, Murphy TL, Spee C, Soriano D, Ishibashi T, Hinton DR, Ryan SJ:
395 Vessel formation by choroidal endothelial cells in vitro is modulated by retinal pigment epithelial
396 cells. *Archives of Ophthalmology* 1995, 113:512-20.
- 397 [15] Geisen P, McColm JR, Hartnett ME: Choroidal endothelial cells transmigrate across the
398 retinal pigment epithelium but do not proliferate in response to soluble vascular endothelial
399 growth factor. *Experimental eye research* 2006, 82:608-19.
- 400 [16] Wang H, Geisen P, Wittchen ES, King B, Burr ridge K, D'Amore PA, Hartnett ME: The role of
401 RPE cell-associated VEGF189 in choroidal endothelial cell transmigration across the RPE.
402 *Investigative ophthalmology & visual science* 2011, 52:570-8.
- 403 [17] Skottman H, Muranen J, Lähdekorpi H, Pajula E, Mäkelä K, Koivusalo L, Koistinen A, Uusitalo
404 H, Kaarniranta K, Juuti-Uusitalo K: Contacting co-culture of human retinal microvascular
405 endothelial cells alters barrier function of human embryonic stem cell derived retinal pigment
406 epithelial cells. *Experimental cell research* 2017, 359:101-11.

- 407 [18] Liu X, Zhu M, Yang X, Wang Y, Qin B, Cui C, Chen H, Sang A: Inhibition of RACK1 ameliorates
408 choroidal neovascularization formation in vitro and in vivo. *Experimental and molecular*
409 *pathology* 2016, 100:451-9.
- 410 [19] Wisniewska-Kruk J, Hoeben KA, Vogels IM, Gaillard PJ, Van Noorden CJ, Schlingemann RO,
411 Klaassen I: A novel co-culture model of the blood-retinal barrier based on primary retinal
412 endothelial cells, pericytes and astrocytes. *Experimental eye research* 2012, 96:181-90.
- 413 [20] Limb GA, Salt TE, Munro PM, Moss SE, Khaw PT: In vitro characterization of a spontaneously
414 immortalized human Muller cell line (MIO-M1). *Investigative ophthalmology & visual science*
415 2002, 43:864-9.
- 416 [21] Vecino E, Rodriguez FD, Ruzafa N, Pereiro X, Sharma SC: Glia–neuron interactions in the
417 mammalian retina. *Progress in retinal and eye research* 2016, 51:1-40.
- 418 [22] Malina KC-K, Cooper I, Teichberg VI: Closing the gap between the in-vivo and in-vitro blood–
419 brain barrier tightness. *Brain research* 2009, 1284:12-21.
- 420 [23] Gerhardinger C, Costa MB, Coulombe MC, Toth I, Hoehn T, Grosu P: Expression of acute-
421 phase response proteins in retinal Muller cells in diabetes. *Investigative ophthalmology & visual*
422 *science* 2005, 46:349-57.
- 423 [24] Zhang SX, Wang JJ, Gao G, Shao C, Mott R, Ma J-x: Pigment epithelium-derived factor (PEDF)
424 is an endogenous antiinflammatory factor. *The FASEB journal* 2006, 20:323-5.
- 425 [25] Yoshida Y, Yamagishi SI, Matsui T, Jinnouchi Y, Fukami K, Imaizumi T, Yamakawa R:
426 Protective role of pigment epithelium-derived factor (PEDF) in early phase of experimental
427 diabetic retinopathy. *Diabetes/metabolism research and reviews* 2009, 25:678-86.
- 428 [26] Fronk AH, Vargis E: Methods for culturing retinal pigment epithelial cells: a review of current
429 protocols and future recommendations. *Journal of tissue engineering* 2016,
430 7:2041731416650838.
- 431 [27] Hollborn M, Jahn K, Limb GA, Kohen L, Wiedemann P, Bringmann A: Characterization of the
432 basic fibroblast growth factor-evoked proliferation of the human Müller cell line, MIO-M1.
433 *Graefe's Archive for Clinical and Experimental Ophthalmology* 2004, 242:414-22.
- 434 [28] Weigel AL, Handa JT, Hjelmeland LM: Microarray analysis of H2O2-, HNE-, or tBH-treated
435 ARPE-19 cells. *Free Radical Biology and Medicine* 2002, 33:1419-32.
- 436 [29] Dunn K, Aotaki-Keen A, Putkey F, Hjelmeland L: ARPE-19, a human retinal pigment epithelial
437 cell line with differentiated properties. *Experimental eye research* 1996, 62:155-70.
- 438 [30] Koirala D, Beranova-Giorgianni S, Giorgianni F: Data-independent proteome analysis of
439 ARPE-19 cells. *Data in brief* 2018, 20:333-6.

440

441

442

443

444

445

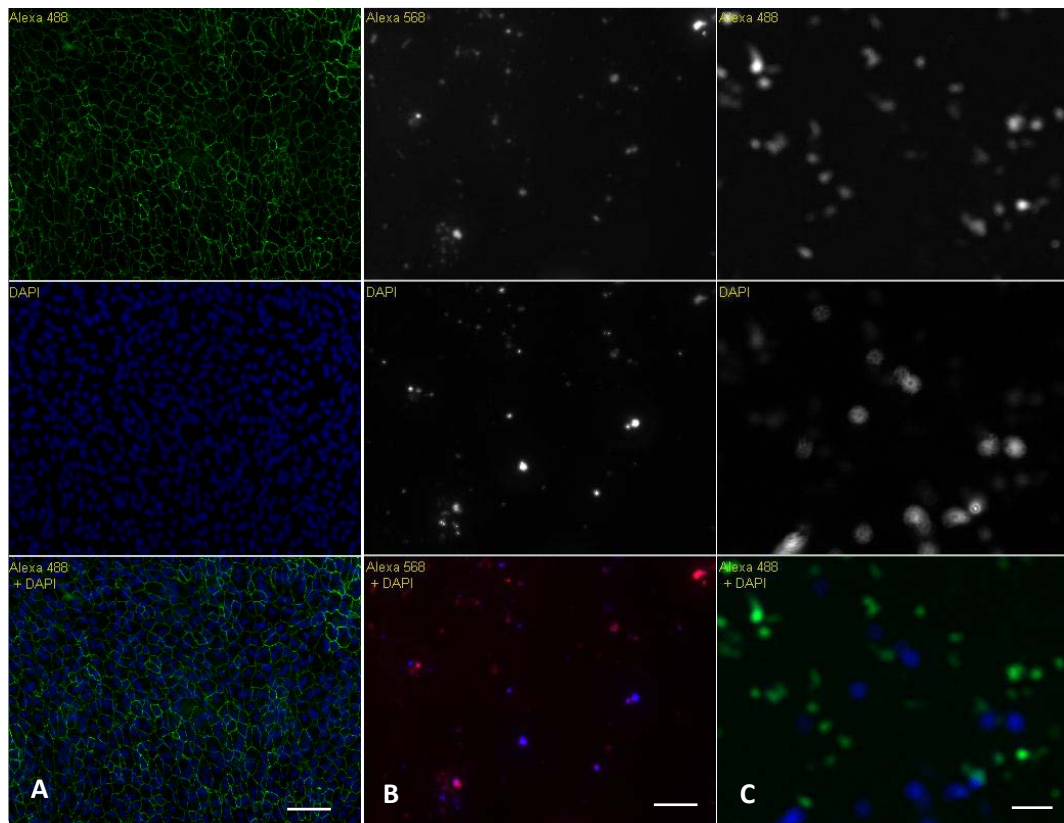
446

447

448 **Supplementary Work**

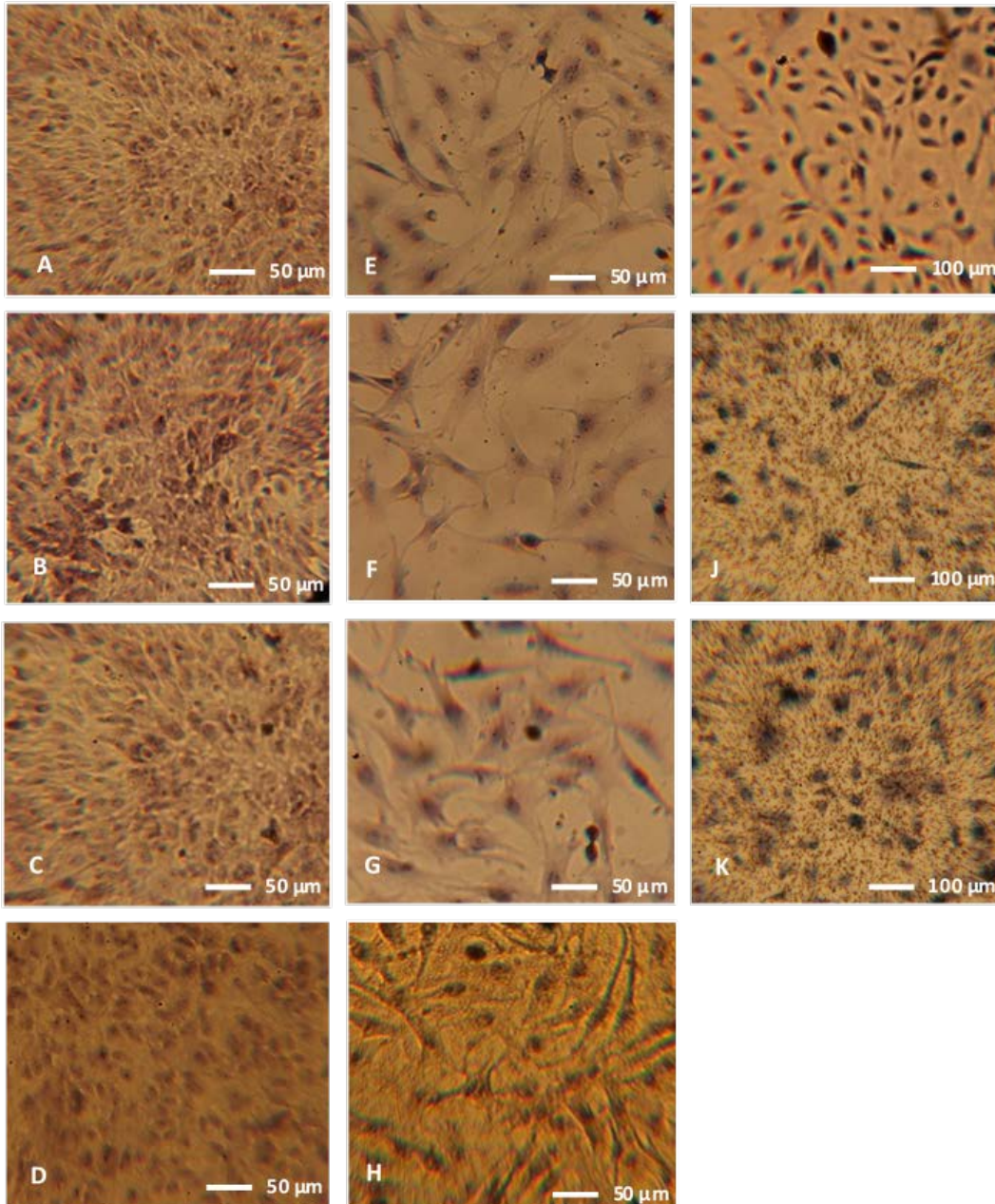
449 **Fluorescent immunocytochemical staining and imaging of cultures**

450 RPE were grown on 0.1% gelatin coated microscope cover slips and left to mature for 28
451 days. Both MIO-M1 and HRMVEC were grown as described on Transwell® membrane.
452 All culture formations (solo, dual and triple) followed the system set up as stated, they
453 were then rinsed in PBS and fixed in ice-cold PBS containing 4% formaldehyde for 30
454 minutes. Cultures were washed with wash buffer (1% BSA in PBS (Sigma Aldrich, UK)),
455 then blocking and permeabilization were achieved by incubation with 5% BSA in 1xPBS
456 with 0.3% Triton X-100 for 40 minutes prior to the addition of primary antibody
457 (prepared in blocking buffer) which was incubated overnight at 4°C. The following
458 conjugated primary antibodies were used: ZO-1 and AlexaFlour 488 (1:100, Thermo
459 Fisher Scientific, UK), Von Willebrand factor and AlexaFlour 594 (1:1500, Novus Bio, UK)
460 and Glutamine synthetase and AlexaFlour 488 (1:500, Novus Bio, UK). Post overnight
461 incubation, cells were washed in wash buffer. This was followed by two washes in PBS
462 and cultures were incubated with 1µg/ml 4', 6'-diamino-2-phenylindole (DAPI; D9542,
463 Sigma Aldrich, UK) for 5 minutes. All cultures were washed an additional two times in
464 PBS and once in deionized H₂O and mounted using PBS and 0.3% Tween-100 as
465 mounting medium (Sigma Aldrich, UK). RPE were mounted straight to slides by inverting
466 coverslips, MIO-M1 and HRMVEC grown on inserts were mounted between two glass
467 coverslips with prior to imaging with a Zeiss microscope with AxioCam MR3 and image
468 analysis with AxioVision 4.6.



469

470 **Sup.Figure 1A-C. Immunocytochemical analysis of cells grown in triple-culture, A- ZO-1 expression in**
 471 **RPE after 28 day maturation marked with Alexa 488 (green), B- Von Willebrand factor expression in**
 472 **HRMVEC grown on the basal side of the membrane marked with Alexa 568 (red), C- Glutamine**
 473 **synthetase expression in MIO-M1 grown on the apical side of the membrane marked with Alexa 488**
 474 **(green). A-C all cells counterstained with nuclear stain DAPI (blue). Scale 50 μ M.**



475

476 **Sup.Figure 2. Representation of Hematoxylin stained cells used in the assessment of cell morphology**
 477 **including analysis of diameter (μM) by ImageJ software. A- RPE solo-culture, B- RPE dual-culture (+MIO-**
 478 **M1), C- RPE dual-culture (+HRMVEC), D- RPE triple-culture, E- MIO-M1 solo-culture, F- MIO-M1 dual-**
 479 **culture (+RPE), G- MIO-M1 dual-culture (+HRMVEC), H- MIO-M1 triple-culture, I- HRMVEC solo-culture,**
 480 **J- HRMVEC dual-culture (+RPE) & K- HRMVEC dual-culture (+MIO-M1).**

481